Original Article

Geometric remodeling of tricuspid valve in pulmonary hypertension and its correlation with pulmonary hypertension severity: a prospectively case-control study using four-dimensional automatic tricuspid valve quantification technology

Yawen Wang[1#], Zhenhui Zhu[1#], Lili Niu[1#], Bingyang Liu[2], Jingru Lin[1], Minjie Lu[3], Changming Xiong[2], Jiangtao Wang[4], Yuqi Cai[1], Hao Wang[1], Weichun Wu[1]

[1]Department of Echocardiography, State Key Laboratory of Cardiovascular Disease, Fuwai Hospital, National Center for Cardiovascular Diseases, Chinese Academy of Medical Sciences and Peking Union Medical College, Beijing, China; [2]Department of Cardiology, Pulmonary Vascular Disease Center, State Key Laboratory of Cardiovascular Disease, Fuwai Hospital, National Center for Cardiovascular Diseases, Chinese Academy of Medical Sciences and Peking Union Medical College, Beijing, China; [3]Department of Magnetic Resonance Imaging, Key Laboratory of Cardiovascular Imaging (Cultivation), Chinese Academy of Medical Sciences, State Key Laboratory of Cardiovascular Disease, Fuwai Hospital, National Center for Cardiovascular Diseases, Chinese Academy of Medical Sciences and Peking Union Medical College, Beijing, China; [4]GE Healthcare, Beijing, China

Contributions: (I) Conception and design: Y Wang, W Wu; (II) Administrative support: M Lu, C Xiong; (III) Provision of study materials or patients: B Liu, C Xiong, W Wu; (IV) Collection and assembly of data: L Niu; (V) Data analysis and interpretation: Y Wang; (VI) Manuscript writing: All authors; (VII) Final approval of manuscript: All authors.

[#]These authors contributed equally to this work as co-first authors.

Correspondence to: Weichun Wu, MD. Department of Echocardiography, State Key Laboratory of Cardiovascular Disease, Fuwai Hospital, Chinese Academy of Medical Sciences and Peking Union Medical College, 167 Beilishi Road, Xicheng District, Beijing 100037, China. Email: achundoctor@163.com.

Background: Evaluation of the tricuspid valve (TV) is crucial for clinical decision making and post-treatment follow-up in pulmonary hypertension (PH) patients. However, little is known about 4-dimensional (4D) TV geometric remodeling in patients with PH. The aim of this study was to examine the 4D geometry of the TV in PH and its correlation with PH severity.

Methods: A total of 74 PH patients with mean pulmonary arterial pressure >25 mmHg and 15 age- and gender-matched healthy individuals were consecutively included from September 2017 to December 2018 in National Center for Cardiovascular Diseases, Fuwai Hospital. All participants underwent 2-dimensional (2D) and 4D transthoracic echocardiography and PH patients underwent right heart catheterization (RHC) within 48 hours of echocardiography. TV geometry was analyzed using a dedicated 4D echocardiography from the right ventricular-focused apical view.

Results: Compared with controls, PH patients had significantly larger 4D tricuspid annular (TA) and TV tenting sizes except in the 2-chamber diameter. In high-quality image cases, maximal tenting height (MTH), coaptation point height, tenting volume and 4-chamber diameter had good or moderate correlation with PH severity graded according to RHC mean pulmonary artery pressure (r=0.705, r=0.644, r=0.602, r=0.472, respectively; P<0.001 for all). In multivariable linear regression analysis, PH severity was independently associated with coaptation point height (F=18.070, P<0.001 with an R^2=0.647) and MTH (F=25.576, P<0.001 with an R^2=0.378). Among all 4D TV parameters, MTH had the highest area under the receiver operating characteristic (ROC) curve (AUC) in high-quality image cases [AUC =0.857, 95% confidence interval (CI): 0.743–0.972; P<0.001], comparable to echocardiographic systolic pulmonary arterial pressure (AUC =0.847, 95% CI: 0.733–0.961; P<0.001).

Conclusions: In PH, TV geometric remodeling occurs mainly in TA septal-lateral dimension and TV tenting height. Worsening PH is an independent determinant of TV coaptation point height and MTH, not TA size. MTH shows a great diagnostic potential to detect severe PH.

Keywords: Pulmonary hypertension (PH); tricuspid valve (TV); 3-dimensional echocardiography (3DE); 4-dimensional echocardiography (4DE)

Submitted Aug 14, 2023. Accepted for publication Dec 05, 2023. Published online Jan 18, 2024.
doi: 10.21037/qims-23-1150
View this article at: https://dx.doi.org/10.21037/qims-23-1150

Introduction

Pulmonary hypertension (PH), which is defined as resting mean pulmonary arterial pressure (mPAP) ≥25 mmHg assessed by right heart catheterization (RHC), affects all age groups with a prevalence of 1% of the global population (1). PH is a pathophysiological disorder associated with worsening symptoms and poor outcomes regardless of the underlying etiology, especially for severe PH (2). In the general pathophysiologic sequence of PH, right ventricular (RV) diastolic dysfunction and right atrial (RA) dilation lead to tricuspid annular (TA) dilatation and tricuspid regurgitation (TR), followed by deterioration of RV pressure and volume overload, which exacerbates PH and RV and tricuspid valve (TV) apparatus remodeling (3-6). The wide use of RCH, the gold-standard method of establishing PH, is limited by its reliance on invasive measurement. Computed tomography (CT) is usually used to identify the cause of PH. Echocardiography is an important and noninvasive modality for screening and follow-up of PH with Doppler echocardiography estimating TR and systolic pulmonary arterial pressure (sPAP) and 2-dimensional (2D) or 3-dimensional (3D) echocardiography validating RV and RA remodeling (2,5). However, echocardiographic markers for geometric remodeling of TV have not been well validated.

Current guidelines for PH recommend that transplantation should continue to be an important option for severe PH (2), and have confirmed the successful performance of combined TV repair and double lung transplantation procedures in severe PH based on RHC without an increase in morbidity or mortality (7). Moreover, patients with a concordant PH diagnosis have been demonstrated to have a similar outcome to patients without PH after transcatheter TV repair (8). Preprocedurally evaluated TV characteristics have been proposed as predictors of procedural success (9,10). However, the geometric changes of TV in patients with PH have not been robustly characterized.

TA is a highly dynamic, complex geometric structure with elliptical and saddle shape displacing toward the atrium in anterior and posterior aspects (11). 3-dimensional echocardiography (3DE) or 4-dimensional echocardiography (4DE), irrespective of its orientation in space, has been confirmed to achieve a more accurate quantification of the TA, avoiding geometric assumptions and plane position errors (5). These findings evoke the hypothesis that 4D automatic tricuspid valve quantification (4D Auto-TVQ) would have the potential to assess the size of the TV systematically. Accordingly, we sought to achieve the following: (I) describe the 4-dimensional (4D) geometry of the TV in a relatively large cohort of PH; (II) explore the relationships between TV remodeling and PH severity based on RHC. We present this article in accordance with the STROBE reporting checklist (available at https://qims.amegroups.com/article/view/10.21037/qims-23-1150/rc).

Methods

Study population

A total of 89 participants including healthy volunteers and patients with PH were consecutively included from September 2017 to December 2018 in National Center for Cardiovascular Diseases, Fuwai Hospital in this prospective case-control study. A flow chart describing the patient selection process is shown in *Figure 1*. Patients were included if they were ≥18 years of age with a mPAP of >25 mmHg, and they had not received any specific therapy before echocardiography. The exclusion criteria were intra-cardiac shunts, atrial fibrillation, significant coronary heart disease, organic TV disease, renal or hepatic failure, PH due to hypoxia or severe left-sided heart disease, and inadequate image quality. The controls comprised

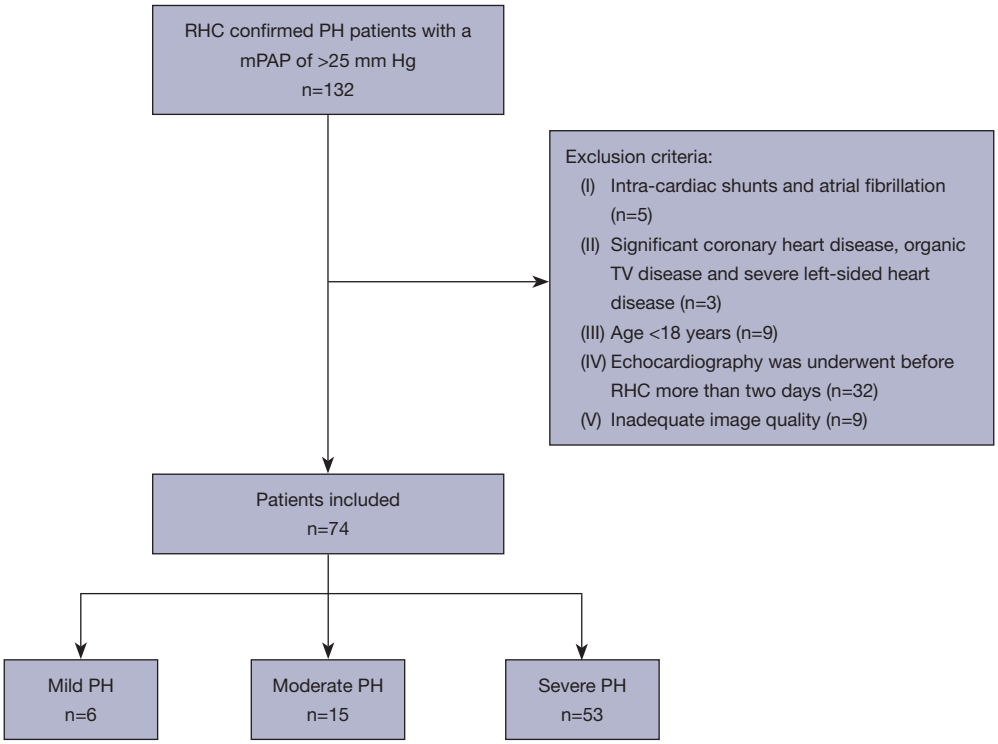

Figure 1 A flow chart of patient selection. RHC, right heart catheterization; PH, pulmonary hypertension; mPAP, mean pulmonary arterial pressure; TV, tricuspid valve.

15 age- and gender-matched healthy individuals with no history of cardiovascular disease and no echocardiographic abnormalities. All patients underwent conventional echocardiography, 4DE, 4D Auto-TVQ analysis, and RHC within 48 hours of image acquisition. This study conformed to the Declaration of Helsinki (as revised in 2013) and was approved by the Ethics Committee of Fuwai Hospital (No. 2018-1063). Informed consent was obtained from each patient.

Conventional echocardiography

All participants underwent a conventional 2-dimensional (2D) transthoracic echocardiographic assessment in accordance with the latest guidelines (12,13), using GE Vivid E9 (GE Healthcare, Milwaukee, WI, USA) with a 3.5-MHz transducer. All images were analyzed offline using dedicated software (EchoPAC 204; GE Healthcare, Horton, Norway). RA and RV size were measured from the focused RV apical view, and fractional area change was calculated [(diastolic area – systolic area)/diastolic area]. Tricuspid annular plane systolic excursion (TAPSE) was measured in the apical 4-chamber view by placing the M-mode cursor through the lateral tricuspid annulus. In the apical 4-chamber view, pulsed-wave Doppler was used to assess the tricuspid inflow between the tricuspid leaflets, and accordingly, the peak E (early diastolic) and A (atrial contraction) velocities were recorded and measured. sPAP was derived from the maximal TR jet velocity and the right atrial pressure (RAP), which was invasively estimated by inferior vena cava size and collapse. The patients with equivalent RA-RV pressures and noneffective echocardiographic sPAP were excluded. The TR severity was graded as mild, moderate, or severe, using the multiparametric approach recommended by the current guidelines (14). All the echocardiographic images were acquired and routinely measured by an operator with the title of deputy chief physician.

4DE

4DE was acquired using the 4V matrix-array transducer on the cardiac ultrasound GE system. Full-volume acquisitions of the TV, RV, and RA were performed from the RV-focused apical view using electrocardiogram gating over

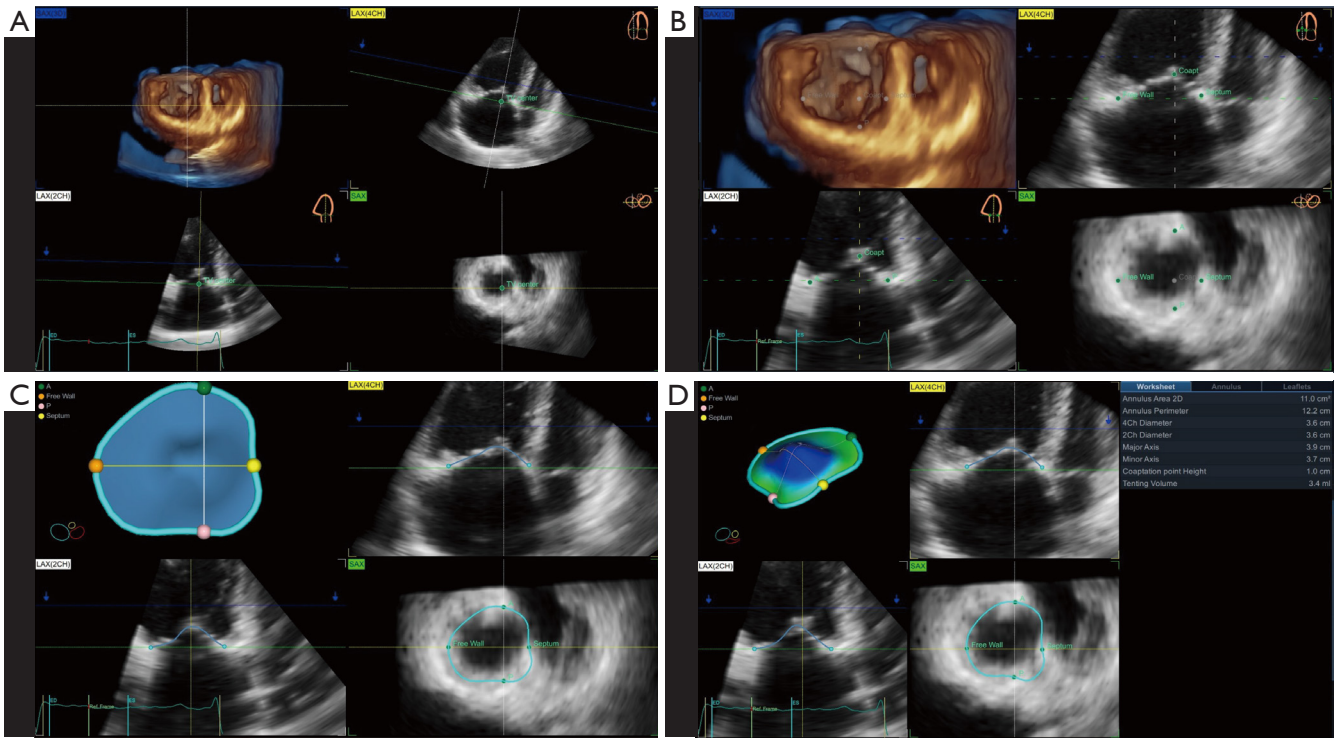

Figure 2 Measurements of TV geometry and function using 4DE and a dedicated commercial software (4D Auto-TVQ). (A) Alignment of the cut planes centered on the TA. (B) Manual selection of the anatomical landmarks. (C) Review and additional changes of automatically generated TV leaflet contours. (D) Surface rendering of the TV and quantitative analysis of its geometry and function. TV, tricuspid valve; 4DE, 4-dimensional echocardiography; TA, tricuspid annular; LAX, long-axis; SAX, short-axis; 4D Auto-TVQ, 4D automatic tricuspid valve quantification.

4–6 consecutive cardiac cycles during a single breath-hold. Gain settings were optimized and temporal resolution was maximized by optimizing sector width and minimizing depth. The frame rate was ≥12 FPS. All 4DE data sets were stored digitally and analyzed offline by the same operator with 5 years of professional experience in echocardiography.

RA and RV quantitative analysis

Right atrial end-systolic volume (RAESV) and right ventricular end-diastolic volume (RVEDV) were measured using a 4DE software package designed for volumetric analysis of the left atrium and right ventricle respectively (4D Auto LAQ and 4D Auto RVQ).

TV quantitative analysis

TV measurements were obtained semi-automatically to quantify TV apparatus morphology and function using dedicated commercial software (4D Auto-TVQ). The algorithm extracted the TA model and tracked it throughout the cardiac cycle by the combination of user-identified TA surface and the deformation of the 3D annular model, then, a 3D configuration of the TV leaflets at the reference frame was constructed using leaflet edge detection. After editing manually, TV measurements were automatically computed. In detail, the 4DE data set was automatically sliced to obtain 3 planes corresponding to the apical 4-chamber view, its respective orthogonal RV longitudinal view, and a transversal cut plane, which were manually adjusted to obtain the view of interest, particularly transversal cut plane (*Figure 2A*). Initialization of the TA was manually performed in mid-systole by identifying the TV leaflet hinge points and the leaflet coaptation point (*Figure 2B*). Further editing was allowed on any user-identified rotational plane (*Figure 2C*). Afterward, the software automatically provided both static and dynamic parameters of the TV geometry (*Figure 2D*). The PH patients were divided into high-quality

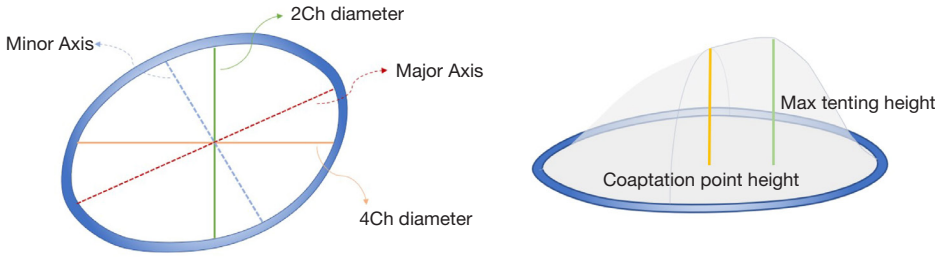

Figure 3 Geometry of the TV and its measurements by 4D Auto-TVQ analysis tool. TV, tricuspid valve; 4D Auto-TVQ, 4D automatic tricuspid valve quantification.

image cases and not-high-quality image cases based on the image tracking throughout the cardiac cycle.

TV parameters were subsequently generated as follows (*Figure 3*): TA area 3D (area of non-planar surface of TA); TV area 2D (the area of 2D valve plane of TA); TA perimeter (the length of the 3D contour); 4-chamber diameter (4Ch diameter, the distance between septal and lateral TV hinge points at mid-systole); 4-chamber diastolic diameter (4Ch Diast diameter, maximum distance between septal and lateral TV hinge points during diastole); 2-chamber diameter (2Ch diameter, the distance between anterior and posterior TV hinge points at mid-systole); major axis (the largest diameter of the TA at mid-systole); major diastolic axis (the largest diameter of the TA during diastole); minor axis (the smallest diameter of the TA at mid-systole); sphericity index (the ratio between the minor and the major diameters); TA excursion (absolute longitudinal displacement of the annulus during the cardiac cycle); TA coaptation point height (distance between the coaptation point and 4-chamber TA annulus diameter); maximal tenting height (MTH; peak distance of the valve surface to the TV plane); and TA tenting volume (volume encompassed by the TV leaflets and the TA surface).

RHC

All patients underwent RHC within 2 days. The catheter was positioned in the right heart cavity and pulmonary artery. Hemodynamic parameters included the mean right atrial pressure (mRAP), right ventricular systolic pressure (RVSP), mean pulmonary artery pressures (mPAP), and pulmonary artery wedge pressure (PAWP). Hemodynamic definition of PH used cut-off values of mPAP ≥25 mmHg, PH severity was graded as mild (25 mmHg ≤ mPAP <35 mmHg), moderate (35 mmHg ≤ mPAP <45 mmHg), or severe (mPAP ≥45 mmHg) in the present study.

Reproducibility of TV measurements

To obtain the interobserver variability, TV measurements were repeated in a randomly selected subgroup of 15 patients by 2 independent blinded observers. Intraobserver variability was assessed by the same observer on the same 15 studies 2 weeks apart.

Statistical analysis

Continuous variables were expressed as mean ± standard deviation (SD) or median with interquartile range (IQR) according to the normal distribution. Categorical variables were expressed as frequencies and percentages. The normal distribution of the data was assessed using the Shapiro-Wilk test. Continuous data were compared using the Student's *t*-test or the Mann-Whitney *U* test, whereas categorical data were analyzed with the χ^2 or Fisher's exact tests. Correlations between TV parameters and PH severity measured by RHC were performed using Spearman's correlation coefficient ($r \geq 0.8$, excellent; $0.5 \leq r < 0.8$, good; $0.3 \leq r < 0.5$, moderate; $r < 0.3$, poor). Univariate linear regression was performed to identify TV apparatus remodeling with RAESV, RVEDV, PH severity, and TR severity. Stepwise linear regression was used for multivariable analysis, testing the hypothesis that PH severity would be independently related to TV MTH after adjusting for covariates. Logistic regression analysis was performed to find the variables associated with severe PH. Receiver operating characteristic (ROC) curve analysis was used to compare the ability of TV parameters and echocardiographic sPAP to predict severe PH. Intra- and inter-observer reproducibility of were assessed by intraclass correlation coefficient and coefficient of variation.

Statistical analysis was performed using SPSS, version 25.0 (IBM Corp., Armonk, NY, USA). All statistical tests were 2-sided, and P<0.05 was considered statistically significant.

Results

Characteristics of the study population

A total of 74 patients with PH and 15 healthy volunteers were included in this study, among whom 51 cases had high-quality images. Characteristics of the study population, including clinical characteristics, hemodynamic results, PH severity, clinical classification, conventional echocardiographic parameters, and 4D RA and RV parameters, are summarized in *Table 1*. The differences of TR grade and echocardiographic sPAP between the 2 groups were significant (P<0.001 for all, *Table 1*). No differences were observed in age and gender between patients with PH and healthy volunteers.

TV parameters

Compared with the normal controls, annulus area and annulus perimeter were significantly larger in PH patients (P=0.001 for both, *Table 2*). 4Ch diameter, major axis, and minor axis had significant differences between the 2 groups (P<0.05 for all, *Table 2*). Coaptation point height, MTH, and tenting volume were significantly higher and TA excursion was significantly lower in patients with PH compared with the normal controls (P<0.001 for all, *Table 2*). The differences of 2Ch diameter, annulus area change and sphericity index between the 2 groups were not significant (P>0.05 for all, *Table 2*).

Correlation between PH severity and 4DE TV characteristics

There were weak but significant correlations between PH severity and TV parameters except annuals area change, 2Ch diameter, major axis, major diastolic axis, and sphericity index in all participants (*Table 3*). In high-quality image cases, MTH had the best correlation with PH severity (r=0.705, P<0.001; *Table 3*). 4Ch diastolic diameter, TA excursion, coaptation point height, and tenting volume all showed good correlations with PH severity (r=0.535, –0.517, 0.644, 0.602, respectively, P<0.001 for all; *Table 3*). In addition, there were also moderate correlations between PH severity with TV parameters: annulus area 3D, annulus perimeter, and minor axis (r=0.388, 0.399, 0.440, respectively, P<0.01 for all; *Table 3*).

Table 1 Clinical, 2DE, and 4D RA and RV characteristics of study population

Parameters	PH (n=74)	Healthy control (n=15)	P value
Age (years)	39.53±12.15	38.40±12.83	0.75
Gender (male)	23 [31.1]	4 [26.7]	0.98
BSA (m^2)	1.60±0.16		
BMI (kg/m^2)	22.64±3.44		
NT-proBNP (pg/mL)	710.50 (340.55–1,720.15)		
6MWD (m)	407.86±94.16		
WHO-FC I/II/III	3/22/31		
Hemodynamics			
mRAP (mmHg)	3.00 (1.00–6.00)		
RVSP (mmHg)	92.38±19.52		
mPAP (mmHg)	53.10±12.10		
PVR ($dyn{\cdot}s{\cdot}cm^{-5}$)	792.19 (572.69–959.11)		
PAWP (mmHg)	7.15±3.57		
RV-CI ($L/min/m^2$)	2.89 (2.34–3.43)		

Table 1 (*continued*)

Table 1 (*continued*)

Parameters	PH (n=74)	Healthy control (n=15)	P value
PH severity			
Mild PH	6 [8]		
Moderate PH	15 [20]		
Severe PH	53 [72]		
Clinical classification			
IPAH	31 [42]		
PH with unclear mechanisms	21 [28]		
CTEPH	13 [18]		
CTD-PAH	7 [9]		
PAH after operation of CHD	2 [3]		
2DE parameters			
RVD (mm)	33.47±7.67	22.27±2.60	<0.001
RAD (mm)	46.40±11.45	34.33±4.16	<0.001
RV-FAC (%)	30.07±9.73	46.33±11.44	<0.001
TAPSE (mm)	16.21±3.26	22.25±2.67	<0.001
TR (m/s)	4.29±0.69	2.02±0.47	<0.001
TR severity mild/moderate/severe	7/0/0	27/13/24	<0.001
TV E/A	1.15±0.44	1.45±0.52	0.04
LVEF (%)	68.77±7.00	68.50±4.60	0.42
Echocardiographic sPAP	81.49±23.22	221.08±8.44	<0.001
4DE parameters			
RAESV (mL)	82.26±45.64	37.25±11.23	<0.001
RVEDV (mL)	135.39±46.58	83.27±27.73	<0.001

Data are presented as mean ± standard deviation, median (interquartile range) or n [%]. 2DE, 2-dimensional echocardiography; 4D, 4-dimensional; RA, right atrial; RV, right ventricular; BSA, body surface area; BMI, body mass index; NT-proBNP, N-terminal pro–brain natriuretic peptide; 6MWD, 6-min walking distance; WHO-FC, World Health Organization functional class; mRAP, mean right atrial pressure; RVSP, right ventricular systolic pressure; mPAP, mean pulmonary arterial pressure; PVR, pulmonary vascular resistance; PAWP, pulmonary wedge artery pressure; RV-CI, right ventricular cardiac index; IPAH, idiopathic pulmonary arterial hypertension; CTEPH, chronic thromboembolic pulmonary hypertension; CTD, connective tissue disease; CHD, congenital heart disease; RVD, right ventricular diameter; RAD, right atrial diameter; FAC, fractional area change; TAPSE, tricuspid annular plane systolic excursion; TR, tricuspid regurgitation velocity; TV E/A, tricuspid valve blood early and atrium flow; LVEF, left ventricular ejection fraction; RAESV, right atrial end-systolic volume; RVEDV, right ventricular end-diastolic volume.

At univariable linear regression analysis in high-quality image cases, the follow TV parameters had strong associations with RAESV, RVEDV, PH severity, and TR severity: annulus area 3D, annulus perimeter, 4Ch diameter, coaptation point height, MTH, and tenting volume (*Table 4*). At stepwise multivariable linear regression analysis, annulus area 3D, annulus perimeter, and 4Ch diameter were independently associated with RAESV and (or) RVEDV and tenting volume was independently associated with RVEDV and TR severity. Coaptation point height was independently associated with PH severity. TV MTH was independently correlated with PH severity and RVEDV

Table 2 TV quantitative parameters of study population

Parameters	PH (n=74)	Healthy control (n=15)	P value
Annulus area 3D (cm^2)	12.37±3.16	9.46±2.41	0.001
Annulus area 2D (cm^2)	12.18±3.11	9.33±2.38	0.001
Annulus area change (%)	15.53±5.80	17.83±6.73	0.18
Annulus perimeter (cm)	12.60±1.58	11.01±1.38	0.001
4Ch diameter (cm)	3.93±0.56	3.31±0.46	<0.001
4Ch diastolic diameter (cm)	4.16±0.60	3.51±0.45	<0.001
2Ch diameter (cm)	3.64±0.53	3.43±0.64	0.17
Major axis (cm)	4.19±0.53	3.81±0.46	0.01
Major diastolic axis (cm)	4.42±0.54	4.09±0.49	0.03
Minor axis (cm)	3.59±0.50	3.07±0.50	<0.001
Sphericity index (%)	83.39±15.34	81.40±10.51	0.63
Excursion (mm)	8.30±2.53	11.60±3.20	<0.001
Coaptation point height (mm)	10.58±3.00	6.20±2.37	<0.001
MTH (mm)	10.26±2.72	6.00±1.25	<0.001
Tenting volume (mL)	3.95±1.94	1.87±0.85	<0.001

Data are presented as mean ± standard deviation. TV, tricuspid valve; PH, pulmonary hypertension; 3D, 3-dimensional; 2D, 2-dimensional; 4Ch diameter, 4-chamber diameter; 2Ch diameter, 2-chamber diameter; MTH, maximal tenting height.

Table 3 Correlation between PH severity and 4DE TV characteristics

Parameters	All cases (n=74)		High-quality image cases (n=51)	
	r	P value	r	P value
Annulus area 3D (cm^2)	0.225	0.03	0.388	0.005
Annulus area 2D (cm^2)	0.220	0.04	0.384	0.005
Annulus area change (%)	0.055	0.61	0.020	0.89
Annulus perimeter (cm)	0.226	0.03	0.399	0.004
4Ch diameter (cm)	0.283	0.007	0.472	<0.001
4Ch diastolic diameter (cm)	0.285	0.007	0.535	<0.001
2Ch diameter (cm)	0.073	0.50	0.139	0.33
Major axis (cm)	0.123	0.25	0.237	0.09
Major diastolic axis (cm)	0.097	0.37	0.240	0.09
Minor axis (cm)	0.253	0.02	0.440	0.001
Sphericity index (%)	0.130	0.22	0.192	0.18
Excursion (mm)	–0.442	<0.001	–0.517	<0.001
Coaptation point height (mm)	0.359	0.001	0.644	<0.001
MTH (mm)	0.411	<0.001	0.705	<0.001
Tenting volume (mL)	0.352	0.001	0.602	<0.001

PH, pulmonary hypertension; 4DE, 4-dimensional echocardiography; TV, tricuspid valve; 3D, 3-dimensional; 2D, 2-dimensional; 4Ch diameter, 4-chamber diameter; 2Ch diameter, 2-chamber diameter; MTH, maximal tenting height.

Table 4 Univariable and multivariate linear regression analysis of RAESV, RVEDV, PH severity, and TR severity used to predict 4DE TV characteristics in high-quality image cases

Variables	Univariable analysis		Multivariate analysis	
	β (95% CI)	P value	β (95% CI)	P value
Annulus area 3D (cm^2)				
RAESV (mL)	0.041 (0.024–0.059)	<0.001		
RVEDV (mL)	0.039 (0.024–0.054)	<0.001	0.042 (0.029–0.056)	<0.001
PH severity	1.037 (0.408–1.667)	0.002		
TR severity	1.437 (0.721–2.153)	<0.001		
Annulus perimeter (cm)				
RAESV (mL)	0.022 (0.012–0.031)	<0.001		
RVEDV (mL)	0.020 (0.012–0.028)	<0.001	0.022 (0.015–0.029)	<0.001
PH severity	0.570 (0.243–0.896)	0.001		
TR severity	0.751 (0.373–1.129)	<0.001		
4Ch diameter (cm)				
RAESV (mL)	0.007 (0.004–0.011)	<0.001	0.007 (0.004–0.011)	<0.001
RVEDV (mL)	0.005 (0.002–0.008)	0.001		
PH severity	0.227 (0.116–0.339)	<0.001		
TR severity	0.199 (0.058–0.340)	0.007		
Coaptation point height (mm)				
RAESV (mL)	0.041 (0.021–0.061)	<0.001		
RVEDV (mL)	0.033 (0.014–0.052)	0.001		
PH severity	1.615 (1.013–2.218)	<0.001	1.691 (1.016–2.366)	<0.001
TR severity	1.357 (0.510–2.204)	0.002		
MTH (mm)				
RAESV (mL)	0.047 (0.031–0.062)	<0.001		
RVEDV (mL)	0.040 (0.026–0.054)	<0.001	0.027 (0.014–0.040)	<0.001
PH severity	1.653 (1.174–2.131)	<0.001	1.188 (0.683–1.694)	<0.001
TR severity	1.882 (1.264–2.500)	<0.001		
Tenting volume (mL)				
RAESV (mL)	0.029 (0.019–0.039)	<0.001		
RVEDV (mL)	0.025 (0.016–0.034)	<0.001	0.020 (0.011–0.029)	<0.001
PH severity	0.814 (0.459–1.168)	<0.001		
TR severity	1.067 (0.649–1.486)	<0.001	0.642 (0.212–1.073)	0.004

PH, pulmonary hypertension; TR, tricuspid regurgitation; 4DE, 4-dimensional echocardiography; TV, tricuspid valve; CI, confidence interval; 4Ch diameter, 4-chamber diameter; RAESV, right atrial end-systolic volume; RVEDV, right ventricular end-diastolic volume; MTH, maximal tenting height.

Table 5 Univariable and multivariate logistic regression analysis of RAESV, RVEDV, coaptation point height, and MTH used to predict severe PH in high-quality image cases

Variables	Univariable analysis		Multivariate analysis	
	OR (95% CI)	P value	OR (95% CI)	P value
RAESV (mL)	1.037 (1.014–1.060)	0.002	1.026 (0.994–1.058)	0.11
RVEDV (mL)	1.013 (1.000–1.027)	0.05	0.979 (0.954–1.004)	0.10
Coaptation point Height (mm)	1.564 (1.172–2.087)	0.002	0.993 (0.604–1.633)	0.98
MTH (mm)	1.764 (1.292–2.407)	<0.001	1.965 (1.004–3.847)	0.049

RAESV, right atrial end-systolic volume; RVEDV, right ventricular end-diastolic volume; MTH, maximal tenting height; PH, pulmonary hypertension; OR, odds ratio; CI, confidence interval.

(F=18.070, P<0.001 with an R^2=0.647). MTH increased by 0.12 cm for each increment in PH severity and by 0.03 cm for each 10 mL increment in RVEDV. In the multivariable logistic regression analysis in high-quality image cases, MTH was the strongest predictor of severe PH [odds ratio (OR) =1.965, P<0.05], compared with RAESV, RVEDV, and TV coaptation point height (OR =1.026, 0.979, 0.993, respectively, P>0.05 for all; *Table 5*).

Prediction of severe PH using 4DE TV characteristics

Using ROC curve analysis, MTH had the largest area under the curve (AUC =0.857) to predict severe PH among all TV parameters and was comparable to TR velocity (AUC =0.830) and echocardiographic sPAP (AUC =0.847) in high-quality image cases. Similarly, coaptation point height (AUC =0.822) and tenting volume (AUC =0.802) had an excellent ability to predict severe PH, whereas 4Ch diastolic diameter during diastole had a relatively smaller AUC (AUC =0.742) (*Table 6*; *Figure 4*). However, in all participants, TR velocity (AUC =0.832) and echocardiographic sPAP (AUC =0.837) were superior to MTH (AUC =0.686) in AUC (*Table 6*).

Intra- and inter-observer variability

All 4DE TV measurements showed excellent intra- and inter-observer reproducibility (*Table 7*).

Discussion

In our study, we explored TV geometry and the relationships between 4DE TV parameters and right heart volumes and PH severity. In this study, we reported that TV coaptation point height and MTH were independently associated with PH severity and could predict severe PH. The main findings of this study can be summarized as follows: (I) PH patients had significantly abnormal TV geometry; (II) PH severity was an independent determinant of 4D TV coaptation point height and MTH; (III) TV MTH was the best parameter to detect severe PH patients among 4D TV parameters and comparable to echocardiographic sPAP, followed by coaptation point height and tenting volume.

The TA in PH patients

Previous studies have shown TA dilation in PH patients (3,15,16). Muraru *et al.* and Guta *et al.* (5,17) reported that TA area was independently correlated with RAESV and RVEDV. Our study also demonstrated that RVEDV or RAESV was an independent factor associated with TA area, TA perimeter, or 4Ch diameter of TA in PH patients. Anatomically, patients with a dilated RV have significant displacement of all papillary muscles away from the center of the annulus, with the anterior papillary muscle displaced laterally and the septal and posterior papillary muscles displaced toward the LV (18). Fukuda *et al.* (19) revealed that the annulus was dilated in the septal to lateral and posteroseptal to anterolateral directions in patients with functional TR. Besides, the RA myocardium anchors the pectinate muscles and surrounds the TV orifice with its thin musculature fibers inserting into the leaflet hinges, which is more predisposed to dilation in the status of PH (20). These mechanics may provide a pathophysiologic basis for the significantly larger area, perimeter, and 4Ch diameter of TA but similar 2Ch diameter of TA in PH patients compared with healthy people. In our study, the difference of sphericity index between PH and healthy volunteers were not significant. We think that this may be due to the proportional increase of major diameter and

Table 6 Performance of 4DE TV characteristics, TR velocity and echocardiographic sPAP for detecting severe PH in high-quality image cases and in all cases

Parameters	AUC	95% CI	P value	Cutoff	Sensitivity (%)	Specificity (%)	Youden index
High-quality image cases (51)							
Annulus area 3D (cm^2)	0.667	0.510–0.823	0.05	12.95	56	79.2	0.352
Annulus area 2D (cm^2)	0.667	0.510–0.823	0.05	12.75	56	79.2	0.352
Annulus area change (%)	0.535	0.369–0.701	0.67	13.65	72	45.8	0.178
Annulus perimeter (cm)	0.669	0.153–0.825	0.04	12.9	56	79.2	0.352
4Ch diameter (cm)	0.708	0.559–0.856	0.01	4.15	60	83.3	0.433
4Ch diastolic diameter (cm)	0.742	0.598–0.885	0.004	4.45	56	83.3	0.393
2Ch diameter (cm)	0.581	0.416–0.746	0.33	3.45	84	45.8	0.298
Major axis (cm)	0.580	0.416–0.744	0.34	3.85	88	37.5	0.255
Major diastolic axis (cm)	0.588	0.423–0.752	0.29	4.45	64	58.3	0.223
Minor axis (cm)	0.697	0.548–0.846	0.02	3.35	84	54.2	0.382
Sphericity index (%)	0.592	0.429–0.754	0.27	84.5	60	62.5	0.225
Excursion (mm)	0.232	0.092–0.373	0.001	5.50	92	8.3	0.003
Coaptation point height (mm)	0.822	0.696–0.947	<0.001	9.50	88	70.8	0.588
MTH (mm)	0.857	0.743–0.972	<0.001	8.50	96	66.7	0.627
Tenting volume (mL)	0.802	0.674–0.929	<0.001	3.95	64	87.5	0.515
TR velocity	0.830	0.712–0.948	<0.001	3.3	96	62.5	0.585
Echocardiographic sPAP	0.847	0.733–0.961	<0.001	77.98	72	87.5	0.595
All cases (74)							
Annulus area 3D (cm^2)	0.596	0.473–0.720	0.13	12.95	44.2	77.1	0.214
Annulus area 2D (cm^2)	0.594	0.470–0.718	0.14	9.75	80.8	40.0	0.208
Annulus area change (%)	0.551	0.424–0.678	0.42	13.55	67.3	48.6	0.159
Annulus perimeter (cm)	0.594	0.470–0.718	0.14	11.45	78.8	42.9	0.217
4Ch diameter (cm)	0.614	0.494–0.734	0.07	3.45	82.7	40.0	0.227
4Ch diastolic diameter (cm)	0.614	0.495–0.734	0.07	4.55	30.8	91.4	0.222
2Ch diameter (cm)	0.555	0.426–0.683	0.39	3.45	71.2	48.6	0.197
Major axis (cm)	0.538	0.411–0.664	0.55	3.85	75.0	40.0	0.150
Major diastolic axis (cm)	0.529	0.404–0.654	0.64	4.45	48.1	60.0	0.081
Minor axis (cm)	0.614	0.491–0.737	0.07	3.35	73.1	54.3	0.274
Sphericity index (%)	0.572	0.447–0.696	0.26	84.5	57.7	60.0	0.177
Excursion (mm)	0.268	0.158–0.378	<0.001	9.50	23.1	37.1	–0.398
Coaptation point height (mm)	0.662	0.539–0.785	0.01	7.50	94.2	37.1	0.314
MTH (mm)	0.686	0.565–0.806	0.003	7.50	86.5	48.6	0.351
Tenting volume (mL)	0.663	0.547–0.780	0.01	2.50	82.7	45.7	0.284
TR velocity	0.832	0.745–0.919	<0.001	4.49	55.8	97.1	0.529
Echocardiographic sPAP	0.837	0.750–9.923	<0.001	74.00	76.9	74.3	0.512

4DE, 4-dimensional echocardiography; TV, tricuspid valve; TR, tricuspid regurgitation; sPAP, systolic pulmonary artery pressure; PH, pulmonary hypertension; AUC, area under the curve; CI, confidence interval; 3D, 3-dimensional; 2D, 2-dimensional; 4Ch diameter, 4-chamber diameter; 2Ch diameter, 2-chamber diameter; MTH, maximal tenting height.

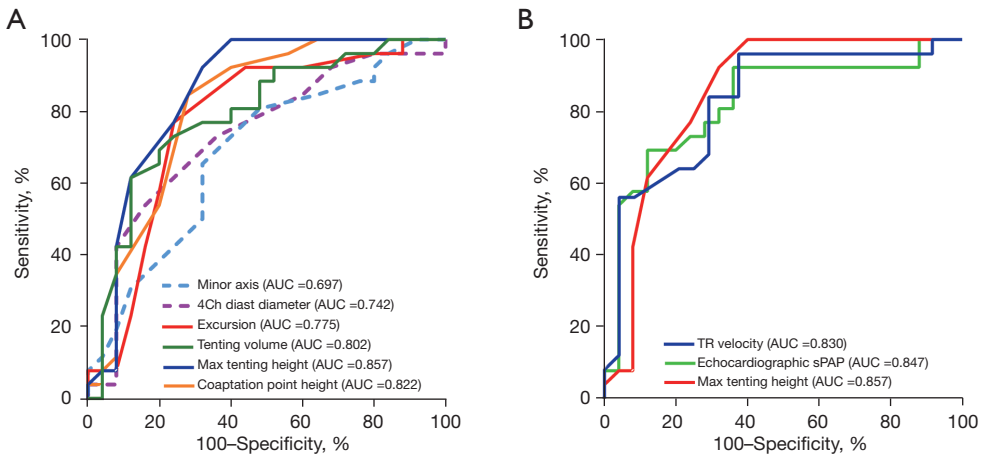

Figure 4 ROC curves of conventional echocardiography and 4D echocardiography to detect severe PH in high-quality image cases. (A) ROC curves of minor axis, 4Ch diastolic diameter, excursion, tenting volume, MTH, and coaptation point height to detect severe PH. (B) ROC curves of TR velocity, echocardiography sPAP, and MTH to detect severe PH. AUC, area under the curve (P<0.05 for all). AUC, area under the curve; TR, tricuspid regurgitation; sPAP, systolic pulmonary arterial pressure; ROC, receiver operator characteristic; 4D, 4-dimensional; MTH, maximal tenting height; PH, pulmonary hypertension.

Table 7 Intra- and interobserver reproducibility of the parameters describing TV geometry

Parameters	Intra-observer		Inter-observer	
	ICC	CV	ICC	CV
Annulus area 3D (cm^2)	0.930	0.19	0.872	0.23
Annulus area 2D (cm^2)	0.930	0.19	0.862	0.23
Annulus area change (%)	0.906	0.30	0.852	0.31
Annulus perimeter (cm)	0.959	0.10	0.929	0.11
4Ch diameter (cm)	0.948	0.12	0.882	0.13
4Ch diastolic diameter (cm)	0.977	0.12	0.900	0.12
2Ch diameter (cm)	0.928	0.10	0.872	0.11
Major axis (cm)	0.949	0.11	0.934	0.12
Major diastolic axis (cm)	0.944	0.08	0.917	0.09
Minor axis (cm)	0.945	0.12	0.860	0.13
Sphericity index (%)	0.911	0.09	0.901	0.09
Excursion (mm)	0.994	0.21	0.985	0.43
Coaptation point height (mm)	0.907	0.23	0.891	0.21
MTH (mm)	0.925	0.22	0.881	0.23
Tenting volume (mL)	0.973	0.36	0.967	0.38

TV, tricuspid valve; ICC, intraclass correlation coefficient; CV, coefficient of variation; 3D, 3-dimensional; 2D, 2-dimensional; 4Ch diameter, 4-chamber diameter; 2Ch diameter, 2-chamber diameter; MTH, maximal tenting height.

minor diameter. Indeed, major axis and minor axis were significantly larger in PH patients in our study. Our results showed that the differences of annulus area change between the 2 groups were not significant. In contrast to previous studies, we were able to measure TA diameter using a dedicated software package developed for the TV, taking into account the nonplanarity of the annulus and provide unique information.

The TV tenting in PH patients

Atrial fibrillation patients with functional TR have increased TA tenting volumes associated with a reduction in the coaptation height (17). In AF patients, TV leaflet tethering is characteristically absent, since the RV basal region is devoid of papillary muscles (5). In contrast, there were larger TV tenting in patients with functional TR secondary to PH, which may be related to ability to grow in size in response to the systolic stress (21). In patients with functional TR secondary to PH, there was a spherical deformation of the right ventricle with increased length and mid-transversal diameter, which causes displacement and re-alignment of the papillary muscles with a consequent TV leaflets tethering (6). Medvedofsky *et al.* (3) also concluded that functional TR progression secondary to PH is associated with elongation of the TV leaflets. Our present study extends these findings and provides firm evidence that enlarged TV tenting height is independently associated with PH severity. PH severity is an independent determinant of TV coaptation point height and MTH. In our study, we also found that TR severity was not independently associated with TV coaptation point height and MTH, which could be explained by the fact that only mild TR was presented in a proportion of severe PH patients (22,23).

Topilsky *et al.* (15) showed that leaflet deformation with increased tenting height is the main determinant of TR effective-regurgitant-orifice in PH. Recent studies have consistently demonstrated that enlarged TV tethering height and tethering volume are associated with adverse clinical outcomes following tricuspid annuloplasty, highlighting the importance of comprehensive assessment of TV tethering (24). According to previous observations, effective reduction of tethering is key to successful TV surgery and annuloplasty alone could not reduce leaflet tethering. The peak tenting site is sometimes difficult to identify by 2DE. It is thus necessary to account for TV tenting by 4DE with angle independent to offer additional and detailed evaluation.

4D MTH to detect severe PH

Elevated mPAP is associated with poor prognosis in PH (25), and Maron *et al.* (26) have gone further by showing that mPAP can independently predict the major clinical events of mortality and heart failure hospitalization. As severe PH patients may actually be severely hemodynamically compromised and at risk of rapid deterioration, prompt management is of considerable importance. A recent guideline suggests that the hemodynamic variable, as an important element, should be considered to evaluate the severity of PH in order to inform therapeutic decisions (27). The 2009 European Society of Cardiology (ESC) and European Respiratory Society (ERS) guidelines for the diagnosis and treatment of PH recommend combination therapy in severe PH patient (28). D'Alto *et al.* (29) and Sitbon *et al.* (30) revealed that upfront triple combination therapy in severe PH patients is associated with considerable clinical and hemodynamic improvement, right-sided heart reverse remodeling, and long-term benefits. Furthermore, an important reduction in pulmonary vascular resistance is the driving mechanism for clinical benefit and improved outcome. Recent studies have demonstrated that a reduction of mPAP, appearing to be a meaningful treatment target, results in favorable outcomes and long-term survival benefit in PH patients (31,32). Thus, accurate diagnosis and classification of PH severity is a pivotal step to clinical decision making, prognosis and post-treatment follow-up.

Echocardiography, as a noninvasive diagnostic investigation, is a Class 1C recommended first line method in cases of suspected PH (2). Moreover, noninvasive echocardiographic estimation of mPAP may be used to follow and monitor treatment effects in patients with definite PH. However, echocardiographic sPAP is a flow-dependent variable and TR peak velocity measurement is angle dependent, the accuracy of echocardiography for estimating sPAP is still controversial (33). Lv *et al.* (34) studied 218 highly suspected PH patients who underwent RHC and echocardiography and found that echocardiographic sPAP tends to be underestimated at a high sPAP level of RHC and echocardiography also tends to underestimate pulmonary artery pressure when pulmonary artery wedge pressure increased. Our research explored the diagnostic potential of 4D TV parameters. The ROC curve demonstrated that 4D MTH without geometric assumptions and plane position errors were most associated with severe PH and comparable to echocardiographic sPAP. However, in all study groups,

4D MTH was inferior to echocardiographic sPAP in detecting severe PH, which may be due to the poor tracking of TV leaflet hinge points and the leaflet coaptation point throughout the cardiac cycle.

Limitation

Our study has several limitations. As a single-center study, there were relatively few patients with potential selection bias. This was mainly as a result of the need of excluding PH due to severe left-sided heart disease or lung disease to avoid the confounding effect of hypoxia and heart failure. A larger multicenter trial with large samples is necessary to confirm our preliminary findings. Besides, the clinical characteristics of healthy volunteers were incomplete, which should be supplemented in further studies. In addition, the TV geometry was assessed using a semi-automated tool based on user-identified landmarks of TA. Therefore, the research results may be influenced by the quality of images, although we have excluded PH patient with inadequate image quality. Moreover, we did not conduct cardiac magnetic resonance imaging and CT, but Muraru *et al.* (35) have tested the accuracy of the measurements of the TA geometry obtained with 4D Auto-TVQ compared to cardiac CT. Also, our study only enrolled PH patients and explored the TV remodeling in PH settings. Due to the limitation of other etiologic settings and the geometry and function of RA and RV, we failed to analyze the TV geometry of different etiologies and the difference between atrial and ventricular functional remodeling in the current study. In the future, we would like to enroll patients with different etiologies, such as left heart disease, corrected tetralogy of Fallot, chronic atrial fibrillation, and so on, and we will further explore the difference between atrial and ventricular functional remodeling in different functional states of TV. Nevertheless, our study assessed the diagnostic potential of 4D TV parameters for identification of severe PH in participants with high-quality images. Finally, several studies have investigated the therapeutic effects in patients with severe PAH mainly based on the World Health Organization functional class (WHO-FC) classification (29,30,36), whereas our study classified the severity of PH based on mPAP.

Conclusions

In PH, TV geometric remodeling is characterized by TA dilatation mainly in the septal-lateral dimension and TV tenting height increasement. The progression of PH classified by mPAP is an independent determinant of TV tenting heigh, suggesting that mPAP could be an important mechanism of TV leaflet tethering irrespective of RAESV and RVEDV in PH. 4D TV MTH also shows a great diagnostic potential to detect severe PH. Awareness of TV tenting height increasement as a consequence of geometric remodeling in patients with PH state and as predictor of severe PH is of potential value for the imaging follow-up and treatment of PH patients.

Acknowledgments

We are indebted to the patients who participated in this study. We thank the research staff and the Department of Cardiology of Fuwai Hospital for their invaluable assistance in this research.

Funding: This work was supported by the Construction Research Project of Key Laboratory (Cultivation) of the Chinese Academy of Medical Sciences (No. 2019PT310025), and Capital Health Development and Scientific Research Projects (No. 2016-2-4036).

Footnote

Reporting Checklist: The authors have completed the STROBE reporting checklist. Available at https://qims.amegroups.com/article/view/10.21037/qims-23-1150/rc

Conflicts of Interest: All authors have completed the ICMJE uniform disclosure form (available at https://qims.amegroups.com/article/view/10.21037/qims-23-1150/coif). J.W. reports that she is an employee of GE Healthcare and provided technical support for this study, and she had no financial or other conflicts with respect to the study. The other authors have no conflicts of interest to declare.

Ethical Statement: The authors are accountable for all aspects of the work in ensuring that questions related to the accuracy or integrity of any part of the work are appropriately investigated and resolved. The study conforms to the Declaration of Helsinki (as revised in 2013) and was approved by the Ethics Committee of Fuwai Hospital (No. 2018-1063). Informed consent was provided by each patient.

References

1. Humbert M, Kovacs G, Hoeper MM, Badagliacca R, Berger RMF, Brida M, et al. 2022 ESC/ERS Guidelines for the diagnosis and treatment of pulmonary hypertension. Eur Heart J 2022;43:3618-731. Erratum in: Eur Heart J 2023;44:1312.
2. Galiè N, Humbert M, Vachiery JL, Gibbs S, Lang I, Torbicki A, et al. 2015 ESC/ERS Guidelines for the diagnosis and treatment of pulmonary hypertension: The Joint Task Force for the Diagnosis and Treatment of Pulmonary Hypertension of the European Society of Cardiology (ESC) and the European Respiratory Society (ERS): Endorsed by: Association for European Paediatric and Congenital Cardiology (AEPC), International Society for Heart and Lung Transplantation (ISHLT). Eur Respir J 2015;46:903-75.
3. Medvedofsky D, Aronson D, Gomberg-Maitland M, Thomeas V, Rich S, Spencer K, Mor-Avi V, Addetia K, Lang RM, Shiran A. Tricuspid regurgitation progression and regression in pulmonary arterial hypertension: implications for right ventricular and tricuspid valve apparatus geometry and patients outcome. Eur Heart J Cardiovasc Imaging 2017;18:86-94.
4. Casa LD, Dolensky JR, Spinner EM, Veledar E, Lerakis S, Yoganathan AP. Impact of pulmonary hypertension on tricuspid valve function. Ann Biomed Eng 2013;41:709-24.
5. Muraru D, Addetia K, Guta AC, Ochoa-Jimenez RC, Genovese D, Veronesi F, Basso C, Iliceto S, Badano LP, Lang RM. Right atrial volume is a major determinant of tricuspid annulus area in functional tricuspid regurgitation: a three-dimensional echocardiographic study. Eur Heart J Cardiovasc Imaging 2021;22:660-9.
6. Florescu DR, Muraru D, Florescu C, Volpato V, Caravita S, Perger E, Bălșeanu TA, Parati G, Badano LP. Right heart chambers geometry and function in patients with the atrial and the ventricular phenotypes of functional tricuspid regurgitation. Eur Heart J Cardiovasc Imaging 2022;23:930-40.
7. Shigemura N, Sareyyupoglu B, Bhama J, Bonde P, Thacker J, Bermudez C, Gries C, Crespo M, Johnson B, Pilewski J, Toyoda Y. Combining tricuspid valve repair with double lung transplantation in patients with severe pulmonary hypertension, tricuspid regurgitation, and right ventricular dysfunction. Chest 2011;140:1033-9.
8. Lurz P, Orban M, Besler C, Braun D, Schlotter F, Noack T, Desch S, Karam N, Kresoja KP, Hagl C, Borger M, Nabauer M, Massberg S, Thiele H, Hausleiter J, Rommel KP. Clinical characteristics, diagnosis, and risk stratification of pulmonary hypertension in severe tricuspid regurgitation and implications for transcatheter tricuspid valve repair. Eur Heart J 2020;41:2785-95.
9. Ancona F, Stella S, Taramasso M, Marini C, Latib A, Denti P, Grigioni F, Enriquez-Sarano M, Alfieri O, Colombo A, Maisano F, Agricola E. Multimodality imaging of the tricuspid valve with implication for percutaneous repair approaches. Heart 2017;103:1073-81.
10. Besler C, Orban M, Rommel KP, Braun D, Patel M, Hagl C, Borger M, Nabauer M, Massberg S, Thiele H, Hausleiter J, Lurz P. Predictors of Procedural and Clinical Outcomes in Patients With Symptomatic Tricuspid Regurgitation Undergoing Transcatheter Edge-to-Edge Repair. JACC Cardiovasc Interv 2018;11:1119-28.
11. Ton-Nu TT, Levine RA, Handschumacher MD, Dorer DJ, Yosefy C, Fan D, Hua L, Jiang L, Hung J. Geometric determinants of functional tricuspid regurgitation: insights from 3-dimensional echocardiography. Circulation 2006;114:143-9.
12. Rudski LG, Lai WW, Afilalo J, Hua L, Handschumacher MD, Chandrasekaran K, Solomon SD, Louie EK, Schiller NB. Guidelines for the echocardiographic assessment of the right heart in adults: a report from the American Society of Echocardiography endorsed by the European Association of Echocardiography, a registered branch of the European Society of Cardiology, and the Canadian Society of Echocardiography. J Am Soc Echocardiogr 2010;23:685-713; quiz 786-8.
13. Mitchell C, Rahko PS, Blauwet LA, Canaday B, Finstuen JA, Foster MC, Horton K, Ogunyankin KO, Palma RA, Velazquez EJ. Guidelines for Performing a Comprehensive Transthoracic Echocardiographic Examination in Adults: Recommendations from the American Society of Echocardiography. J Am Soc Echocardiogr 2019;32:1-64.
14. Zoghbi WA, Adams D, Bonow RO, Enriquez-Sarano M, Foster E, Grayburn PA, Hahn RT, Han Y, Hung J, Lang RM, Little SH, Shah DJ, Shernan S, Thavendiranathan P, Thomas JD, Weissman NJ. Recommendations for Noninvasive Evaluation of Native Valvular

Regurgitation: A Report from the American Society of Echocardiography Developed in Collaboration with the Society for Cardiovascular Magnetic Resonance. J Am Soc Echocardiogr 2017;30:303-71.
15. Topilsky Y, Khanna A, Le Tourneau T, Park S, Michelena H, Suri R, Mahoney DW, Enriquez-Sarano M. Clinical context and mechanism of functional tricuspid regurgitation in patients with and without pulmonary hypertension. Circ Cardiovasc Imaging 2012;5:314-23.
16. Sukmawan R, Watanabe N, Ogasawara Y, Yamaura Y, Yamamoto K, Wada N, Kume T, Okura H, Yoshida K. Geometric changes of tricuspid valve tenting in tricuspid regurgitation secondary to pulmonary hypertension quantified by novel system with transthoracic real-time 3-dimensional echocardiography. J Am Soc Echocardiogr 2007;20:470-6.
17. Guta AC, Badano LP, Tomaselli M, Mihalcea D, Bartos D, Parati G, Muraru D. The Pathophysiological Link between Right Atrial Remodeling and Functional Tricuspid Regurgitation in Patients with Atrial Fibrillation: A Three-Dimensional Echocardiography Study. J Am Soc Echocardiogr 2021;34:585-594.e1.
18. Spinner EM, Lerakis S, Higginson J, Pernetz M, Howell S, Veledar E, Yoganathan AP. Correlates of tricuspid regurgitation as determined by 3D echocardiography: pulmonary arterial pressure, ventricle geometry, annular dilatation, and papillary muscle displacement. Circ Cardiovasc Imaging 2012;5:43-50.
19. Fukuda S, Saracino G, Matsumura Y, Daimon M, Tran H, Greenberg NL, Hozumi T, Yoshikawa J, Thomas JD, Shiota T. Three-dimensional geometry of the tricuspid annulus in healthy subjects and in patients with functional tricuspid regurgitation: a real-time, 3-dimensional echocardiographic study. Circulation 2006;114:I492-8.
20. Ho SY, Anderson RH, Sánchez-Quintana D. Atrial structure and fibres: morphologic bases of atrial conduction. Cardiovasc Res 2002;54:325-36.
21. Afilalo J, Grapsa J, Nihoyannopoulos P, Beaudoin J, Gibbs JS, Channick RN, Langleben D, Rudski LG, Hua L, Handschumacher MD, Picard MH, Levine RA. Leaflet area as a determinant of tricuspid regurgitation severity in patients with pulmonary hypertension. Circ Cardiovasc Imaging 2015. doi: 10.1161/CIRCIMAGING.114.002714.
22. Mutlak D, Aronson D, Lessick J, Reisner SA, Dabbah S, Agmon Y. Functional tricuspid regurgitation in patients with pulmonary hypertension: is pulmonary artery pressure the only determinant of regurgitation severity? Chest 2009;135:115-21.
23. Lancellotti P, Pibarot P, Chambers J, La Canna G, Pepi M, Dulgheru R, Dweck M, Delgado V, Garbi M, Vannan MA, Montaigne D, Badano L, Maurovich-Horvat P, Pontone G, Vahanian A, Donal E, Cosyns B; Scientific Document Committee of the European Association of Cardiovascular Imaging. Multi-modality imaging assessment of native valvular regurgitation: an EACVI and ESC council of valvular heart disease position paper. Eur Heart J Cardiovasc Imaging 2022;23:e171-232.
24. Chen Y, Liu YX, Yu YJ, Wu MZ, Lam YM, Sit KY, Chan DT, Ho CK, Ho LM, Fang LG, Zhang SY, Lau CP, Au WK, Tse HF, Yiu KH. Prognostic Value of Tricuspid Valve Geometry and Leaflet Coaptation Status in Patients Undergoing Tricuspid Annuloplasty: A Three-Dimensional Echocardiography Study. J Am Soc Echocardiogr 2019;32:1516-25.
25. Khirfan G, Li M, Wang X, Dweik RA, Heresi GA, Tonelli AR. Is pulmonary vascular resistance index better than pulmonary vascular resistance in predicting outcomes in pulmonary arterial hypertension? J Heart Lung Transplant 2021;40:614-22.
26. Maron BA, Brittain EL, Hess E, Waldo SW, Barón AE, Huang S, Goldstein RH, Assad T, Wertheim BM, Alba GA, Leopold JA, Olschewski H, Galiè N, Simonneau G, Kovacs G, Tedford RJ, Humbert M, Choudhary G. Pulmonary vascular resistance and clinical outcomes in patients with pulmonary hypertension: a retrospective cohort study. Lancet Respir Med 2020;8:873-84.
27. Taichman DB, Ornelas J, Chung L, Klinger JR, Lewis S, Mandel J, Palevsky HI, Rich S, Sood N, Rosenzweig EB, Trow TK, Yung R, Elliott CG, Badesch DB. Pharmacologic therapy for pulmonary arterial hypertension in adults: CHEST guideline and expert panel report. Chest 2014;146:449-75.
28. Galiè N, Hoeper MM, Humbert M, Torbicki A, Vachiery JL, Barbera JA, Beghetti M, Corris P, Gaine S, Gibbs JS, Gomez-Sanchez MA, Jondeau G, Klepetko W, Opitz C, Peacock A, Rubin L, Zellweger M, Simonneau G; ESC Committee for Practice Guidelines (CPG). Guidelines for the diagnosis and treatment of pulmonary hypertension: the Task Force for the Diagnosis and Treatment of Pulmonary Hypertension of the European Society of Cardiology (ESC) and the European Respiratory Society (ERS), endorsed by the International Society of Heart and Lung Transplantation (ISHLT). Eur Heart J 2009;30:2493-537. Erratum in: Eur Heart J 2011;32:926.
29. D'Alto M, Badagliacca R, Argiento P, Romeo E, Farro A, Papa S, Sarubbi B, Russo MG, Vizza CD, Golino P, Naeije

R. Risk Reduction and Right Heart Reverse Remodeling by Upfront Triple Combination Therapy in Pulmonary Arterial Hypertension. Chest 2020;157:376-83.
30. Sitbon O, Jaïs X, Savale L, Cottin V, Bergot E, Macari EA, Bouvaist H, Dauphin C, Picard F, Bulifon S, Montani D, Humbert M, Simonneau G. Upfront triple combination therapy in pulmonary arterial hypertension: a pilot study. Eur Respir J 2014;43:1691-7.
31. Sugiyama Y, Matsubara H, Shimokawahara H, Ogawa A. Outcome of mean pulmonary arterial pressure-based intensive treatment for patients with pulmonary arterial hypertension. J Cardiol 2022;80:432-40.
32. Badagliacca R, Vizza CD, Lang I, Sadushi-Kolici R, Papa S, Manzi G, Filomena D, Ogawa A, Shimokawahara H, Matsubara H. Pulmonary pressure recovery in idiopathic, hereditary and drug and toxin-induced pulmonary arterial hypertension: determinants and clinical impact. Vascul Pharmacol 2022;146:107099.
33. Bossone E, D'Andrea A, D'Alto M, Citro R, Argiento P, Ferrara F, Cittadini A, Rubenfire M, Naeije R. Echocardiography in pulmonary arterial hypertension: from diagnosis to prognosis. J Am Soc Echocardiogr 2013;26:1-14.
34. Lv GJ, Li AL, Tao XC, Zhai YN, Zhang Y, Lei JP, Gao Q, Xie WM, Zhai ZG. The accuracy and influencing factors of Doppler echocardiography in estimating pulmonary artery systolic pressure: comparison with right heart catheterization: a retrospective cross-sectional study. BMC Med Imaging 2022;22:91.
35. Muraru D, Gavazzoni M, Heilbron F, Mihalcea DJ, Guta AC, Radu N, Muscogiuri G, Tomaselli M, Sironi S, Parati G, Badano LP. Reference ranges of tricuspid annulus geometry in healthy adults using a dedicated three-dimensional echocardiography software package. Front Cardiovasc Med 2022;9:1011931.
36. Sandoval J, Gaspar J, Peña H, Santos LE, Córdova J, del Valle K, Rodríguez A, Pulido T. Effect of atrial septostomy on the survival of patients with severe pulmonary arterial hypertension. Eur Respir J 2011;38:1343-8.

Cite this article as: Wang Y, Zhu Z, Niu L, Liu B, Lin J, Lu M, Xiong C, Wang J, Cai Y, Wang H, Wu W. Geometric remodeling of tricuspid valve in pulmonary hypertension and its correlation with pulmonary hypertension severity: a prospectively case-control study using four-dimensional automatic tricuspid valve quantification technology. Quant Imaging Med Surg 2024;14(2):1699-1715. doi: 10.21037/qims-23-1150

